Title

The impact of chromosomal translocation locus and fusion oncogene coding sequence in synovial sarcomagenesis.

Journal

Oncogene, 35(38)

ISSN

0950-9232

Authors

Jones, KB
Barrott, JJ
Xie, M
et al.

Publication Date

2016-09-01

DOI

10.1038/onc.2016.38

Peer reviewed

HHS Public Access

Author manuscript

Oncogene. Author manuscript; available in PMC 2016 September 23.

Published in final edited form as:

Oncogene. 2016 September 22; 35(38): 5021–5032. doi:10.1038/onc.2016.38.

The impact of chromosomal translocation locus and fusion oncogene coding sequence in synovial sarcomagenesis

Kevin B. Jones[1,2,3,*], **Jared J. Barrott**[1,2,3], **Mingchao Xie**[4], **Malay Haldar**[5], **Huifeng Jin**[1,2,3], **Ju-Fen Zhu**[1,2,3], **Michael J. Monument**[1,3], **Tim L. Mosbruger**[3,6], **Ellen M. Langer**[5], **R. Lor Randall**[1,3], **Richard K. Wilson**[4,7,8,9], **Bradley R. Cairns**[2,3,10], **Li Ding**[4,7,8,9], and **Mario R. Capecchi**[5]

[1]Department of Orthopaedics, University of Utah, Salt Lake City, Utah 84112, USA

[2]Department of Oncological Sciences, University of Utah, Salt Lake City, Utah 84112, USA

[3]Huntsman Cancer Institute, University of Utah, Salt Lake City, Utah 84112, USA

[4]Department of Medicine, Washington University, St. Louis, Missouri 63108, USA

[5]Department of Human Genetics, University of Utah, Salt Lake City, Utah, USA

[6]Deparment of Bioinformatics, University of Utah, Salt Lake City, Utah, 84112, USA

[7]McDonnell Genome Institute, Washington University, St. Louis, Missouri 63108, USA

[8]Department of Genetics, Washington University, St. Louis, Missouri 63108, USA

[9]Siteman Cancer Center, Washington University, St. Louis, Missouri 63108, USA

[10]Howard Hughes Medical Institute, University of Utah, Salt Lake City, UT 84112, USA

Abstract

Synovial sarcomas are aggressive soft-tissue malignancies that express chromosomal translocation-generated fusion genes, *SS18-SSX1* or *SS18-SSX2* in most cases. Here, we report a mouse sarcoma model expressing *SS18-SSX1*, complementing our prior model expressing *SS18-SSX2*. Exome sequencing identified no recurrent secondary mutations in tumors of either genotype. Most of the few mutations identified in single tumors were present in genes that were minimally or not expressed in any of the tumors. Chromosome 6, either entirely or around the fusion gene expression locus, demonstrated a copy number gain in a majority of tumors of both genotypes. Thus, by fusion oncogene coding sequence alone, *SS18-SSX1* and *SS18-SSX2* can each drive comparable synovial sarcomagenesis, independent from other genetic drivers. *SS18-SSX1* and *SS18-SSX2* tumor transcriptomes demonstrated very few consistent differences overall.

[*]**Contact:** Kevin B. Jones, 2000 Circle of Hope Drive, Room 4263, Salt Lake City, UT 84112, (801) 585-0300, (801) 585-7084 fax, kevin.jones@hci.utah.edu.

Supplementary Information: 3 Supplementary Figures, 7 Supplementary Tables, Supplementary Detailed Methods. All sequencing raw data are available on the SRA PRJNA247995 and GEO GSE71843.

Conflict of Interest

The authors declare no competing financial interests.

In direct tumorigenesis comparisons, *SS18-SSX2* was slightly more sarcomagenic than *SS18-SSX1*, but equivalent in its generation of biphasic histologic features. Meta-analysis of human synovial sarcoma patient series identified two tumor-gentoype-phenotype correlations that were not modeled by the mice, namely a scarcity of male hosts and biphasic histologic features among *SS18-SSX2* tumors. Re-analysis of human *SS18-SSX1* and *SS18-SSX2* tumor transcriptomes demonstrated very few consistent differences, but highlighted increased native *SSX2* expression in *SS18-SSX1* tumors. This suggests that the translocated locus may drive genotype-phenotype differences more than the coding sequence of the fusion gene created. Two possible roles for native SSX2 in synovial sarcomagenesis are explored. Thus even specific partial failures of mouse genetic modeling can be instructive to human tumor biology.

Keywords

genetic mouse model; RNAseq; transcriptome; exome sequencing

Introduction

Synovial sarcoma is the most common soft-tissue sarcoma in young adults and adolescents[1]. Although more responsive to cytotoxic chemotherapy than some other sarcomas, synovial sarcoma proves to be ultimately resistant to most therapies and is usually fatal after metastasis. Synovial sarcoma cells have been shown consistently to bear a balanced t(X;18) chromosomal translocation[2] that generates a fusion between *SS18* (formerly called *SYT*) and an *SSX* gene[3].

Almost the entire *SS18* coding sequence is included in each fusion, while only the final 78 amino acids of SSX1 or SSX2 are included[4,5] By sequence analysis, members of the *SSX* gene family are projected to be transcriptional repressors (Supplementary Fig. 1); their expression is limited to the testis and a few cancers; and little more is known about them beyond their involvement in synovial sarcoma fusions[6–8]. SS18 has been shown to be a member of the mammalian SWI/SNF complex[9,10].

Epigenetic mechanisms have been described wherein SS18-SSX fusion oncoproteins serve as master regulators of transcription in synovial sarcoma cell lines[10,11]. These mechanisms led to the hypothesis that *SS18-SSX* fusion genes were singular driving genetic events in synovial sarcomagenesis[12]. This hypothesis has been supported by limited comparative genomic hybridization and sequencing data that identified few copy number variations and mutations in most synovial sarcomas[13–15].

SS18-SSX2 expression in certain cell lineages proved to be sufficient to drive synovial sarcomagenesis in the mouse at 100 percent penetrance[16,17]. This was initially accepted as circumstantial proof that few or no other genetic changes were necessary for transformation. However, direct comparisons with two other sarcomagenic fusion oncogenes, *EWSR1-ATF1* and *ASPSCR1-TFE3* (related to clear cell and alveolar soft part sarcoma, respectively) demonstrated that *SS18-SSX2* generated fewer sarcomas at longer latencies[18,19]. This suggested that *SS18-SSX2*-driven sarcomagenesis may require some secondary genetic hit

or that the fusion itself was simply less oncogenic. This redirected attention toward *SS18-SSX1*.

Early clinical series comparing *SS18-SSX1* to *SS18-SSX2* found the former to be more common and to associate with higher stage at presentation and worse prognosis[20–24]. Some subsequent series contradict this claim and a recent meta-analysis found no strong statistical evidence for it[25], but the possibility of differential sarcomagenic potential was directly testable in the mouse.

Results

Comparable conditional mouse alleles of *SS18-SSX1* and *SS18-SSX2* expression

To investigate its oncogenic potential, we generated a mouse allele that conditionally expressed the *SS18-SSX1* cDNA from the *Rosa26* locus (termed *hSS1*, Fig. 1a). Using identical primers to capture the full-length coding sequence and early 3' untranslated region, this *hSS1* allele matched the previously described allele for *SS18-SSX2* (herein termed *hSS2*)[16]. Mouse embryonic fibroblasts (MEFs) isolated from each model and exposed in culture to TATCre expressed their respective fusion genes (Fig. 1b) and underwent apoptosis (Fig. 1c). Similarly, both *hSS1* and *hSS2* disrupted early embryogenesis following expression induced by *Hprt-Cre* (Fig. 1d). Thus, *hSS1* and *hSS2* were similarly conditional and toxic to cells in most contexts.

SS18-SSX1 expression in mesenchymal progenitors drives synovial sarcomagenesis

Similar to prior reports with *hSS2*[16], mice were bred to activate *hSS1* in the *Myf5-Cre* lineage. Tumors arose in full penetrance and expressed the fusion gene, as evidenced by fluorescence due to green fluorescent protein (GFP) expression from an internal ribosomal entry site on the targeted construct (Fig. 1e and 1a).

Synovial sarcomas are sub-classified histologically as monophasic synovial sarcoma (MSS), which lacks areas of epithelial differentiation, or biphasic synovial sarcoma (BSS), which contains both fibrous/mesenchymal and epithelial areas. Comparable both to human synovial sarcomas and to *hSS2* mouse tumors, *hSS1*-driven tumors had both histologic types represented (Fig. 1f). As BSS histology indicates a fundamental reprogramming of germ-layer cellular identities from mesenchymal origin to mucinous glandular structure formation, this is considered a diagnostic hallmark unique to synovial sarcoma. Finally, *hSS1* tumors demonstrated the typical immunohistochemical staining with nuclear TLE1, cytoplasmic BCL2, and patchy epithelial membrane antigen and pan-cytokeratin (Fig. 1g). *SS18-SSX1* is therefore also a fusion oncogene capable of driving synovial sarcomagenesis in the mouse.

Synovial sarcoma exomes have few somatic mutations, none recurrent by fusion type

In order to test the genetic independence of each fusion oncogene, we sequenced *Myf5-Cre*-initiated tumor exomes for secondary mutations and compared them to germline control exomes. Few somatic mutations were identified (Fig. 2, Supplementary Tables 1 and 2). Targeted, deeper sequencing was used for validation of all mutations that had an allelic fraction of at least 10% in the tumor and no more than a single read in the germline control

tissue. Most identified mutations demonstrated variant allele fractions well below 40 percent, which in light of the greater than 85 percent typical histologically-determined tumor cell density in the samples, suggests that the mutations were sub-clonal across the neoplasm and therefore had not contributed to initial malignant transformation.

Transcriptome sequencing demonstrated that most mutations also arose in genes that were minimally expressed in the mutated-allele-bearing tumor and minimally expressed in the other tumors that lacked the mutation. This supports their role as likely passenger mutations. Mutant transcript reads were only present as a large fraction of the reads that crossed the mutation site in genes that were minimally expressed overall. Notably, comparison of *hSS1*- and *hSS2*-induced tumors found a slight increase in the number of these passenger mutations in the former, which also developed and were harvested at an older age (Mean 262 versus 168 days).

Mouse synovial sarcomas frequently amplify the fusion expression locus

Exome sequencing was also analyzed to determine copy number variation across the genome. The only repeated copy number variation was in mouse chromosome 6, which was amplified either completely as a trisomy or partially in 24 of the 29 tumors (Fig. 3a–b). The portion of chromosome 6 that was amplified always included the *Rosa26* locus (Fig. 3a–b). PCR was used to test 8 samples with noted amplification and found that the targeted allele, from which the fusion was expressed, was amplified in every case relative to the wildtype allele (Fig. 3c). Comparative genomic hybridization was performed on an additional 11 tumors of the *hSS2* genotype, from 3 different mice, showing the same trisomy of chromosome 6 in 7 of the tumors (Supplementary Fig. 2), with no other consistent changes. Thus, the only genetic change that frequently contributes to mouse synovial sarcomagenesis is amplification of part or all of chromosome 6, consistently including the fusion gene expression locus.

Synovial sarcoma transcriptomes do not consistently differ by fusion genotype

In order to achieve a detailed molecular comparison of synovial sarcomas driven by each fusion genotype, we compared transcriptomes (RNAseq) for tumors of each genotype initiated by *Myf5-Cre*. Unsupervised hierarchical clustering yielded some intermingling of *hSS1* and *hSS2* tumors (Fig. 4a). Just over one thousand genes were differentially expressed between the two tumor genotypes at the $p < 0.05$ significance and 2-fold-change threshold (Supplementary Table 3). As a validation cohort, transcriptomes from 6 tumors initiated by TATCre injection into the hindlimb (3 of each fusion genotype) were also sequenced, with 152 genes differentially expressed to the same degree (Fig. 4b, Supplementary Table 4). Only 18 genes were found to be shared as differentially expressed to the same degree and direction in both comparisons (Fig. 4c–e).

Comparable oncogenesis from *SS18-SSX1* and *SS18-SSX2* in the mouse

To directly compare their oncogenic potential, we developed comparative mouse cohorts of *hSS1* and *hSS2*, each induced by *Myf5-Cre*, *Rosa26-CreER*, or hindlimb injection of the protein TATCre[16,17,26]. In each induction model, *hSS1* expression resulted in slightly fewer, but comparably located tumors, at longer latencies (Fig. 5a–c).

In the *Myf5-Cre*-induced mice, smaller tumors in both genotypes were MSS and rarely included epithelial areas. The *Myf5-Cre;hSS2* mice more often had smaller, secondary tumors identified following euthanasia prompted by a larger tumor, rendering a non-significant decrease in BSS prevalence in that group, overall (p=0.33, Fisher exact test; Fig. 5d). Analysis following stratification of tumors by size found equivalent prevalence of BSS histology in tumors >1 cm, irrespective of fusion genotype (Fig. 5d). The prevalence of BSS histology in tumors initiated by *Rosa26-CreER* and TATCre injection was also not significantly different (p=1.0 and p = 0.58, respectively; Fig. 5d).

Re-analysis of human synovial sarcomas identifies two genotype-phenotype correlations

Early human patient series correlated the *SS18-SSX1* fusion genotype with worse prognosis. Some subsequent series have cast doubt on this. A meta-analysis found the impact to be subtle and not statistically significant. The prevalence of each fusion genotype has also varied somewhat between series.

To focus more clearly on differences associated with each fusion genotype, we retrieved raw data from 1181 patients in 17 of the largest clinical series of human synovial sarcomas in which the fusion type was identified by reverse transcriptase polymerase chain reaction (RT-PCR). Gender data were available from 1036 patients in 12 of the studies. The typical sarcoma male to female ratio of approximately 1.2:1 was reflected among *SS18-SSX1*-expressing tumors pooled from the available series (Table 1). A greater than 1.4-fold shift in gender prevalence was apparent in *SS18-SSX2*-expressing tumors (Table 1). There are significantly fewer males with *SS18-SSX2* tumors than *SS18-SSX1* tumors.

Some clinical series of human synovial sarcomas have reported more rare BSS histology in *SS18-SSX2* tumors, compared to *SS18-SSX1* tumors[21,22,27]. We compared the prevalence of BSS histology in each fusion genotype across the assembled 17 series. This demonstrated a statistically significant reduction in BSS histology cases in synovial sarcomas of the *SS18-SSX2* fusion genotype ($p < 0.0001$, Fisher exact test; Supplementary Table 5).

BSS histology in the *SS18-SSX2* fusion genotype was also tested for gender association. The ratio of male to female biphasic tumors among those expressing *SS18-SSX1* was 1.6-fold higher than the ratio among tumors expressing *SS18-SSX2* (Supplementary Table 6). Four series, including the largest, reported zero male patients with *SS18-SSX2* BSSs.

These data pointed toward two genotype-phenotype relationships in human tumors that were not recapitulated in the mouse, reduced prevalence of male hosts to and BSS histology in *SS18-SSX2* tumors.

Human *SS18-SSX2* synovial sarcomas have reduced native *SSX* gene expression

To identify transcriptional differences between human tumors of each fusion genotype that were not represented in the mouse tumor genotype-expression profile comparisons, we re-analyzed two patient series with reported microarray expression data. To avoid histologic bias, we limited initial comparisons to the pre-treatment MSS tumor samples in each cohort. Few genes had significant differential expression (with matched direction of change) between *SS18-SSX1* and *SS18-SSX2* tumors in both cohorts (Fig. 6a). When these were

cross-referenced to a third group of human samples (a relapsed tumors group from one of the two series), very few genes were significantly different in all three comparisons (Fig. 6a–b). None of these correlated with the genes identified from the mouse comparisons. In particular, the *SSX* genes were prominently represented in the human comparisons, all more highly expressed in *SS18-SSX1* tumors..

We designed RT-qPCR primer sets that targeted the 5' end of either *SSX1* or *SSX2*, portions not included in the respective fusion transcripts. This RT-qPCR analysis of expression in a panel of human synovial sarcomas demonstrated that tumors almost universally expressed native *SSX2*, but detectably expressed *SSX1* in only about half of tumors (Fig. 6c). The only tumor with negligible native *SSX2* expression was the single male case of an *SS18-SSX2*-expressing MSS. The only tumor with higher *SSX1* expression than *SSX2* expression was in a female and was also driven by *SS18-SSX2*. *SSX2* trended toward higher expression in *SS18-SSX1* tumors (Fig. 6d).

This discrepancy in *SSX* gene expression between *SS18-SSX1* and *SS18-SSX2* human tumors was not recapitulated in mouse tumors. Expression of the known members of the homologous mouse *Ssx* gene family were not different between tumors of the two genotypes by RT-qPCR (Supplementary Figure 3a). In the mice, however, the fusion genes were expressed from cDNAs in the *Rosa26* locus, which did not include structural rearrangements of the *Ssx* gene cluster on the X chromosome (Supplementary Figure 3b). Human synovial sarcomas therefore have two important differences between the translocations that generate the *SS18-SSX1* and *SS18-SSX2* fusion genotypes. First, the t(X;18) translocation in a human synovial sarcoma disrupts one allele of the involved, native *SSX* gene, whose 3' exons it repurposes in the fusion gene. This could be especially impactful in males, in which the fusion disrupts the only copy of the involved *SSX* gene. Second, because *SSX2* is oriented away from all the other *SSX* genes, translocation to *SSX2* does not bring any of the other native *SSX* genes into the area of influence of any regional chromatin effects of the high expression *SS18* locus (Supplementary Figure 3c). This contrasts sharply to translocations in *SSX1*, which places most of the *SSX* genes, and *SSX2* in particular, downstream and in close proximity to *SS18*.

Possible roles for native *SSX2* in synovial sarcoma

The model systems for *in vitro* glandular differentiation of human synovial sarcoma cells are not developed yet and the mouse *Ssx* gene family homology to humans is not gene-specific enough to test BSS histology or basic tumorigenesis dependence on *SSX2 in vivo*. We are therefore left to only hypothesis-generating experiments to explain a role for the loss of native SSX2 in either reduced synovial sarcomas in males or reduced BSS histology.

Knock-down of *SSX2* expression by small interfering RNA (siRNA) in human synovial sarcoma cell lines hampered proliferation compared to a non-target control siRNA (Fig. 7a–e). Proliferation increased upon introduction of an *SSX2* overexpression vector compared to control conditions (Fig. 7d–e). These data suggest that SSX2 may function as a contributing oncogene in synovial sarcoma.

Analysis of 3 cohorts of human synovial sarcomas, comparing BSS to MSS tumors in each, identified very few genes with consistent differential expression (Fig. 7f). The most significant among these was the *RAB3IP* gene (Fig. 7g), which encodes one of only two proteins known to interact with SSX2 specifically. The interaction domain is not included in the portion of SSX2 fused to SS18 in the fusion oncoprotein.

Discussion

We report a new model of synovial sarcomagenesis in the mouse, driven by conditional expression of *SS18-SSX1*, complementing our former *SS18-SSX2* model[16]. Exome sequencing demonstrated a striking absence of mutations that by allele fraction and gene transcription levels likely contributed to synovial sarcomagenesis. Although many mouse models of cancer demonstrate lower mutational burdens than their human counterparts, these mouse synovial sarcomas had particularly low mutation numbers per tumor[28–34].

The only recurrent genetic change in tumors, beyond the activation of the *hSS1* or *hSS2* fusion gene, was amplification of part or all of chromosome 6. Mouse tumors more frequently than human tumors demonstrate whole chromosome gains and losses[35,36]. While chromosome 6 trisomy may impact many genes, the partial chromosomal gains always included the *Rosa26* locus and every copy number gain was an increase in the targeted allele. This indicates that increased expression of the fusion may contribute to oncogenesis. The increased expression by copy number gain is likely an artifact of expression from other than the native *Ss18* locus. Indeed, the fact that one *Ss18* allele is not disrupted by translocation may even emphasize the importance of increased expression of the fusion in the mice. The SS18-SSX fusion oncoprotein has been shown to compete with native SS18 for participation in the SWI/SNF complex[10]. The mouse tumors must express enough of the fusion to out-compete two functional alleles of native *Ss18*.

These data suggest that mutations beyond activation and possible amplification of the fusion oncogene are not strictly necessary to enable synovial sarcomagenesis in the appropriate cell of origin in the mouse. Beyond the t(X;18) chromosomal translocation, additional genetic derangements that have been identified in a minority of human synovial sarcomas[13,15] may contribute to tumor progression or make up for a less than ideal cell of origin.

Because SS18-SSX fusion oncogenes are capable of driving synovial sarcomagenesis independently, the details of each fusion genotype and differences between them might engender significant phenotypic differences in tumors. While a recent meta-analysis found no strong statistical justification for increased aggressiveness or worse prognosis in human *SS18-SSX1* tumors[25], our more detailed analysis of all the available human series confirmed that male hosts and BSS histology are specifically rare in the *SS18-SSX2* genotype. In our direct comparison in mice, *SS18-SSX2* was slightly more sarcomagenic than *SS18-SSX1* (and equal between genders) and generated BSS histology equivalently. Therefore, these represented two genotype-phenotype relationships in human synovial sarcoma that expression of each fusion in mice failed to recapitulate. Each demanded explanation.

Each may derive purely from species differences between mouse and human. However, dismissal of these as species-specific modeling failures does not acknowledge one critical character of each departure. In the mouse, *SS18-SSX2* drives more—not less—of synovial sarcoma biology than is apparent from human tumor epidemiology. In mice, there is no large subpopulation of males that do not develop tumors. There is no failure to develop the quintessential synovial sarcoma biology that reprograms mesenchymal cells to organize into the epithelial mucinous glandular structures of BSS histology. The model fails only to limit or partly block each of these biologies as is apparent in human *SS18-SSX2* tumor epidemiology. Rather than species-specific differences in the response to each fusion genotype, therefore, it may relate instead to other artifacts of the model, particularly that expression of a cDNA of the fusion oncogene produced by a chromosomal translocation does not model the other genetic and epigenetic effects of the translocation on the genes near the translocated locus.

This alternate hypothesis that emphasizes the translocation locus effects was supported by the fact that *SSX* gene expression is almost the only differential expression between the two human tumor genotypes that is maintained across multiple patient series. It is also supported by the demonstration that human tumors almost universally express native *SSX2* in addition to the fusion and that *SS18-SSX1* tumors express more *SSX2* than tumors of the *SS18-SSX2* fusion genotype. The fact that both tumorigenesis and BSS histology seem to be limited more profoundly in males also fits with an effect mediated by loss of native *SSX2*, on the X-chromosome.

Generally, X-linkage is considered only in germline heritable traits, due to inactivation of one X chromosome in each female somatic cell. Three points prompt its consideration in this somatic disorder: (1) The inactive X-chromosome in a female cell could be involved in the translocation itself. (2) Many genes on the inactive X chromosome in any female somatic cell are still expressed, escaping imprinting[37]. (3) The *SSX* genes are cancer/testis antigens, only expressed normally in the testis and remaining epigenetically silenced in all other cells unless pathologically activated in certain cancers[7,8]. Thus, whether residing on an active or inactive X chromosome, the *SSX* loci must be epigenetically reactivated to be expressed in a cancer arising outside the testis. A female cell will have two copies of each *SSX* locus physically available for such reactivation. Because *SSX2B*, a locus in opposite orientation but on the same arm of the X chromosome (Supplementary Fig. 3c), codes for the same protein as *SSX2*, female cells will have three copies and male cells will have one copy of the coding sequence available after the translocation that generates *SS18-SSX2*. The existence of *SSX2B* may explain the incomplete/subtle X-linkage of *SSX2*, evidenced by the non-zero prevalence of males with *SS18-SSX2* tumors, generally, and even biphasic tumors in some series.

Demonstrating that modulation of SSX2 levels impacts proliferation in human synovial sarcoma cell lines suggests that *SSX2* may function as an oncogene. Such a role has been demonstrated in other cancers, such as breast cancer, melanoma, and osteosarcoma[38,39]. Certainly, prospective experiments are warranted, as the capacity to generate translocations and assay transformation and tumorgenesis from them in normal human cells *in vitro* are developed.

A role for native SSX2 in the *de novo* gland formation that is characteristic of BSS histology in synovial sarcomas will be even more difficult to test experimentally. Identification of *RAB3IP* as not only among, but most significant within the small group of genes differentially expressed consistently between three comparisons of BSS to MSS histology in human synovial sarcomas, was surprising. The SSX2 protein pulled down RAB3IP specifically in a yeast two-hybrid assay, whereas SSX1 did not[40]. The described interaction domain is in the portion of SSX2 not included in the fusion oncoprotein. A guanine exchange factor for RAB8, the protein encoded by the *RAB3IP* gene, often called Rabin8, has been shown to be important in gland initiation and ciliogenesis[41–43]. How SSX2 may impact these functions remains to be investigated once models are available.

We have therefore shown in mice that both *SS18-SSX1* and *SS18-SSX2* are capable of independently driving synovial sarcomagenesis. Insofar as these models test the impact of each fusion oncogene alone, we find no important tumor phenotypic differences. The differences we confirm epidemiologically in human tumors of the *SS18-SSX2* translocation genotype we hypothesize to be related to the translocation locus rather than the fusion gene generated.

Materials and Methods

A Supplementary Detailed Methods section presents more specifics on each method utilized.

Study Design

Experimental designs were controlled laboratory experiments or depended on either data already collected or specimens already collected and previously reported and indicatedP. The only randomization employed was in manipulations applied to wells of cultured cells, which was done systematically, without any opportunity for bias. Individuals assessing outcomes of histology or cell counts were always blinded as to the group assignment of the specimen being analyzed. Sample size was not pre-calculated by power analysis as the inputs of sample variance were not known *a priori* for most experiments. For other experiments, there was a limited sample size available as subjects from the reported literature, such as in Table 1. Series were excluded from that analysis if gender data or *SS18-SSX* genotype data was not reported and was not retrievable from the original corresponding authors. Otherwise, all data were included from each experiment reported. Outlier data points were not excluded from any analysis. Replicates for each cell line experiment are noted in the figure legends. Blinding was used for all assessments that included the potential for bias on the part of the assessor, such as histology and imaging.

Mice

All mouse work was performed with the approval of the institutional animal care and use committee and in accordance with international legal and ethical norms. The mice bearing *Rosa26*-targeted conditional *SS18-SSX2*, were previously described[16], as were *Rosa26-CreER*[44], *Myf5-Cre*[16] and *Hprt-Cre*[45] mice. The full length cDNA of *SS18-SSX1* was reverse transcribed from total RNA isolated from a human synovial sarcoma sample procured with approval of the institutional review board. Primers were identical to those

used for the prior isolation of *SS18-SSX2*[16]. In all cases, mouse strains were maintained on a mixed C57BL/6 and SvJ background. Littermates were used for comparison controls, whenever possible. The sex of animals was equivalently male and female and not intentionally varied in any group.

Whole exome sequencing

Libraries were prepared using the Sure Select Mouse All Exon kit (Agilent Technologies) for exome enrichment. Paired-end (2×100bp) sequencing was performed with an Illumina HiSeq 2000 instrument. Reads were aligned to the UCSC mm9 mouse reference (derived from NCBI Mouse Build 37) with BWA (version 0.5.9 with parameters -t 4 -q 5). Tumor sample DNA sequencing was compared to paired germline control samples via a somatic variation pipeline using Samtools, Varscan, GATK and Pindel. IDT Targeted Sequencing was performed to validate somatic variants, with read coverage averaging 349.3±124.2.

Transcriptome sequencing

cDNA libraries were constructed using polyA for capture and sequenced on a 50bp single end read run on an Illumina HiSeq 2000 instrument. These were aligned onto UCSC mm9 with CuffLinks software. Differential expression was calculated from read counts using DeSeq2 software.

Clinical Series

We retrieved the raw data from 17 of the largest clinical series of human synovial sarcomas in which the fusion type was identified by reverse transcriptase polymerase chain reaction (RT-PCR)[20–24,46–57]

With the approval of the institutional review board at the University of Utah and in accordance within all international legal and ethical standards, tissue samples from histologically and molecularly confirmed synovial sarcoma patients were procured after obtaining informed consent.

Expression Data

Raw data from Gene Expression Omnibus accession GSE20196 and GSE54187 were downloaded and analyzed using DChip software[58].

Supplementary Material

Refer to Web version on PubMed Central for supplementary material.

Acknowledgments

The authors thank Matt Hockin for provision of the TATCre and Marc Ladanyi, Louis Guillo, Jean-Michel Coindre, Fernanda Amary, Alessandro Gronchi, Ira Koković, Satoshi Takenaka, and Takafumi Ueda for sharing raw data from their previously published patient series. This work was directly supported by the Paul Nabil Bustany Memorial Fund for Synovial Sarcoma Research and the Damon Runyon Cancer Research Foundation to K.B.J., National Cancer Institute / National Institutes of Health (NCI/NIH) grant R01CA180006 to L.D., and National Human Genome Research Institute / NIH grants U01HG006517 to L.D. and U54HG003079 to R.K.W. K.B.J. received additional career development support from NCI/NIH K08CA138764. This work was also partly supported by P30CA042014 from the National Cancer Institute and the Huntsman Cancer Foundation.

References

1. Herzog CE. Overview of sarcomas in the adolescent and young adult population. J Pediatr Hematol Oncol. 2005; 27(4):215–218. [PubMed: 15838394]
2. Turc-Carel C, Dal Cin P, Limon J, Rao U, Li FP, Corson JM, et al. Involvement of chromosome X in primary cytogenetic change in human neoplasia: nonrandom translocation in synovial sarcoma. Proc Natl Acad Sci U S A. 1987; 84(7):1981–1985. [PubMed: 3031659]
3. de Leeuw B, Balemans M, Olde Weghuis D, Geurts van Kessel A. Identification of two alternative fusion genes, SYT-SSX1 and SYT-SSX2, in t(X;18)(p11.2;q11.2)-positive synovial sarcomas. Hum Mol Genet. 1995; 4(6):1097–1099. [PubMed: 7655467]
4. Clark J, Rocques PJ, Crew AJ, Gill S, Shipley J, Chan AM, et al. Identification of novel genes, SYT and SSX, involved in the t(X;18)(p11.2;q11.2) translocation found in human synovial sarcoma. Nat Genet. 1994; 7(4):502–508. [PubMed: 7951320]
5. Crew AJ, Clark J, Fisher C, Gill S, Grimer R, Chand A, et al. Fusion of SYT to two genes, SSX1 and SSX2, encoding proteins with homology to the Kruppel-associated box in human synovial sarcoma. EMBO J. 1995; 14(10):2333–2340. [PubMed: 7539744]
6. Chen YT, Alpen B, Ono T, Gure AO, Scanlan MA, Biggs WH 3rd, et al. Identification and characterization of mouse SSX genes: a multigene family on the X chromosome with restricted cancer/testis expression. Genomics. 2003; 82(6):628–636. [PubMed: 14611804]
7. Gure AO, Tureci O, Sahin U, Tsang S, Scanlan MJ, Jager E, et al. SSX: a multigene family with several members transcribed in normal testis and human cancer. Int J Cancer. 1997; 72(6):965–971. [PubMed: 9378559]
8. Gure AO, Wei IJ, Old LJ, Chen YT. The SSX gene family: characterization of 9 complete genes. Int J Cancer. 2002; 101(5):448–453. [PubMed: 12216073]
9. Perani M, Ingram CJ, Cooper CS, Garrett MD, Goodwin GH. Conserved SNH domain of the proto-oncoprotein SYT interacts with components of the human chromatin remodelling complexes, while the QPGY repeat domain forms homo-oligomers. Oncogene. 2003; 22(50):8156–8167. [PubMed: 14603256]
10. Kadoch C, Crabtree GR. Reversible disruption of mSWI/SNF (BAF) complexes by the SS18-SSX oncogenic fusion in synovial sarcoma. Cell. 2013; 153(1):71–85. [PubMed: 23540691]
11. Su L, Sampaio AV, Jones KB, Pacheco M, Goytain A, Lin S, et al. Deconstruction of the SS18-SSX fusion oncoprotein complex: insights into disease etiology and therapeutics. Cancer cell. 2012; 21(3):333–347. [PubMed: 22439931]
12. Sandberg AA, Bridge JA. Updates on the cytogenetics and molecular genetics of bone and soft tissue tumors. Synovial sarcoma. Cancer genetics and cytogenetics. 2002; 133(1):1–23. [PubMed: 11890984]
13. Barretina J, Taylor BS, Banerji S, Ramos AH, Lagos-Quintana M, Decarolis PL, et al. Subtype-specific genomic alterations define new targets for soft-tissue sarcoma therapy. Nat Genet. 2010; 42(8):715–721. [PubMed: 20601955]
14. Przybyl J, Sciot R, Wozniak A, Schoffski P, Vanspauwen V, Samson I, et al. Metastatic potential is determined early in synovial sarcoma development and reflected by tumor molecular features. The international journal of biochemistry & cell biology. 2014; 53:505–513. [PubMed: 24842110]
15. Joseph CG, Hwang H, Jiao Y, Wood LD, Kinde I, Wu J, et al. Exomic analysis of myxoid liposarcomas, synovial sarcomas, and osteosarcomas. Genes, chromosomes & cancer. 2014; 53(1): 15–24. [PubMed: 24190505]
16. Haldar M, Hancock JD, Coffin CM, Lessnick SL, Capecchi MR. A conditional mouse model of synovial sarcoma: insights into a myogenic origin. Cancer cell. 2007; 11(4):375–388. [PubMed: 17418413]
17. Haldar M, Hedberg ML, Hockin MF, Capecchi MR. A CreER-based random induction strategy for modeling translocation-associated sarcomas in mice. Cancer Res. 2009; 69(8):3657–3664. [PubMed: 19351831]
18. Goodwin ML, Jin H, Straessler K, Smith-Fry K, Zhu JF, Monument MJ, et al. Modeling alveolar soft part sarcomagenesis in the mouse: a role for lactate in the tumor microenvironment. Cancer cell. 2014; 26(6):851–862. [PubMed: 25453902]

19. Straessler KM, Jones KB, Hu H, Jin H, van de Rijn M, Capecchi MR. Modeling clear cell sarcomagenesis in the mouse: cell of origin differentiation state impacts tumor characteristics. Cancer cell. 2013; 23(2):215–227. [PubMed: 23410975]

20. Amary MF, Berisha F, Bernardi Fdel C, Herbert A, James M, Reis-Filho JS, et al. Detection of SS18-SSX fusion transcripts in formalin-fixed paraffin-embedded neoplasms: analysis of conventional RT-PCR, qRT-PCR and dual color FISH as diagnostic tools for synovial sarcoma. Mod Pathol. 2007; 20(4):482–496. [PubMed: 17334349]

21. Guillou L, Benhattar J, Bonichon F, Gallagher G, Terrier P, Stauffer E, et al. Histologic grade, but not SYT-SSX fusion type, is an important prognostic factor in patients with synovial sarcoma: a multicenter, retrospective analysis. J Clin Oncol. 2004; 22(20):4040–4050. [PubMed: 15364967]

22. Ladanyi M, Antonescu CR, Leung DH, Woodruff JM, Kawai A, Healey JH, et al. Impact of SYT-SSX fusion type on the clinical behavior of synovial sarcoma: a multi-institutional retrospective study of 243 patients. Cancer Res. 2002; 62(1):135–140. [PubMed: 11782370]

23. Mezzelani A, Mariani L, Tamborini E, Agus V, Riva C, Lo Vullo S, et al. SYT-SSX fusion genes and prognosis in synovial sarcoma. Br J Cancer. 2001; 85(10):1535–1539. [PubMed: 11720441]

24. Takenaka S, Ueda T, Naka N, Araki N, Hashimoto N, Myoui A, et al. Prognostic implication of SYT-SSX fusion type in synovial sarcoma: a multi-institutional retrospective analysis in Japan. Oncol Rep. 2008; 19(2):467–476. [PubMed: 18202796]

25. Kubo T, Shimose S, Fujimori J, Furuta T, Ochi M. Prognostic value of SS18-SSX fusion type in synovial sarcoma; systematic review and meta-analysis. SpringerPlus. 2015; 4:375. [PubMed: 26217552]

26. Barrott JJ, Illum BE, Jin H, Zhu JF, Mosbruger T, Monument MJ, et al. beta-catenin stabilization enhances SS18-SSX2-driven synovial sarcomagenesis and blocks the mesenchymal to epithelial transition. Oncotarget. 2015; 6(26):22758–22766. [PubMed: 26259251]

27. Kawai A, Woodruff J, Healey JH, Brennan MF, Antonescu CR, Ladanyi M. SYT-SSX gene fusion as a determinant of morphology and prognosis in synovial sarcoma. N Engl J Med. 1998; 338(3): 153–160. [PubMed: 9428816]

28. Francis JC, Melchor L, Campbell J, Kendrick H, Wei W, Armisen-Garrido J, et al. Whole-exome DNA sequence analysis of Brca2- and Trp53-deficient mouse mammary gland tumours. The Journal of pathology. 2015

29. Kim SK, Nasu A, Komori J, Shimizu T, Matsumoto Y, Minaki Y, et al. A model of liver carcinogenesis originating from hepatic progenitor cells with accumulation of genetic alterations. International journal of cancer Journal international du cancer. 2014; 134(5):1067–1076. [PubMed: 23959426]

30. McFadden DG, Papagiannakopoulos T, Taylor-Weiner A, Stewart C, Carter SL, Cibulskis K, et al. Genetic and clonal dissection of murine small cell lung carcinoma progression by genome sequencing. Cell. 2014; 156(6):1298–1311. [PubMed: 24630729]

31. Varela I, Klijn C, Stephens PJ, Mudie LJ, Stebbings L, Galappaththige D, et al. Somatic structural rearrangements in genetically engineered mouse mammary tumors. Genome biology. 2010; 11(10):R100. [PubMed: 20942901]

32. Wartman LD, Larson DE, Xiang Z, Ding L, Chen K, Lin L, et al. Sequencing a mouse acute promyelocytic leukemia genome reveals genetic events relevant for disease progression. The Journal of clinical investigation. 2011; 121(4):1445–1455. [PubMed: 21436584]

33. Westcott PM, Halliwill KD, To MD, Rashid M, Rust AG, Keane TM, et al. The mutational landscapes of genetic and chemical models of Kras-driven lung cancer. Nature. 2015; 517(7535): 489–492. [PubMed: 25363767]

34. Yuan W, Stawiski E, Janakiraman V, Chan E, Durinck S, Edgar KA, et al. Conditional activation of Pik3ca(H1047R) in a knock-in mouse model promotes mammary tumorigenesis and emergence of mutations. Oncogene. 2013; 32(3):318–326. [PubMed: 22370636]

35. Le Roy H, Ricoul M, Ogata H, Apiou F, Dutrillaux B. Chromosome anomalies in mammary carcinoma from transgenic WAPRAS mice: compression with human data. Genes, chromosomes & cancer. 1993; 6(3):156–160. [PubMed: 7682100]

36. Ogawa K, Osanai M, Obata M, Ishizaki K, Kamiya K. Gain of chromosomes 15 and 19 is frequent in both mouse hepatocellular carcinoma cell lines and primary tumors, but loss of chromosomes 4

and 12 is detected only in the cell lines. Carcinogenesis. 1999; 20(11):2083–2088. [PubMed: 10545409]

37. Carrel L, Willard HF. X-inactivation profile reveals extensive variability in X-linked gene expression in females. Nature. 2005; 434(7031):400–404. [PubMed: 15772666]
38. Chen L, Zhou WB, Zhao Y, Liu XA, Ding Q, Zha XM, et al. Cancer/testis antigen SSX2 enhances invasiveness in MCF-7 cells by repressing ERalpha signaling. Int J Oncol. 2012; 40(6):1986–1994. [PubMed: 22344619]
39. D'Arcy P, Maruwge W, Wolahan B, Ma L, Brodin B. Oncogenic functions of the cancer-testis antigen SSX on the proliferation, survival, and signaling pathways of cancer cells. PLoS One. 2014; 9(4):e95136. [PubMed: 24787708]
40. de Bruijn DR, dos Santos NR, Kater-Baats E, Thijssen J, van den Berk L, Stap J, et al. The cancer-related protein SSX2 interacts with the human homologue of a Ras-like GTPase interactor, RAB3IP, and a novel nuclear protein, SSX2IP. Genes, chromosomes & cancer. 2002; 34(3):285–298. [PubMed: 12007189]
41. Breslin A, Denniss FA, Guinn BA. SSX2IP: an emerging role in cancer. Biochemical and biophysical research communications. 2007; 363(3):462–465. [PubMed: 17904521]
42. Hori A, Peddie CJ, Collinson LM, Toda T. Centriolar satellite- and hMsd1/SSX2IP-dependent microtubule anchoring is critical for centriole assembly. Molecular biology of the cell. 2015; 26(11):2005–2019. [PubMed: 25833712]
43. Hur K, Cejas P, Feliu J, Moreno-Rubio J, Burgos E, Boland CR, et al. Hypomethylation of long interspersed nuclear element-1 (LINE-1) leads to activation of proto-oncogenes in human colorectal cancer metastasis. Gut. 2014; 63(4):635–646. [PubMed: 23704319]
44. Badea TC, Wang Y, Nathans J. A noninvasive genetic/pharmacologic strategy for visualizing cell morphology and clonal relationships in the mouse. J Neurosci. 2003; 23(6):2314–2322. [PubMed: 12657690]
45. Tang SH, Silva FJ, Tsark WM, Mann JR. A Cre/loxP-deleter transgenic line in mouse strain 129S1/SvImJ. Genesis. 2002; 32(3):199–202. [PubMed: 11892008]
46. Begueret H, Galateau-Salle F, Guillou L, Chetaille B, Brambilla E, Vignaud JM, et al. Primary intrathoracic synovial sarcoma: a clinicopathologic study of 40 t(X;18)-positive cases from the French Sarcoma Group and the Mesopath Group. Am J Surg Pathol. 2005; 29(3):339–346. [PubMed: 15725802]
47. Ren T, Lu Q, Guo W, Lou Z, Peng X, Jiao G, et al. The clinical implication of SS18-SSX fusion gene in synovial sarcoma. Br J Cancer. 2013; 109(8):2279–2285. [PubMed: 24022186]
48. Sun Y, Sun B, Wang J, Cai W, Zhao X, Zhang S, et al. Prognostic implication of SYT-SSX fusion type and clinicopathological parameters for tumor-related death, recurrence, and metastasis in synovial sarcoma. Cancer Sci. 2009; 100(6):1018–1025. [PubMed: 19385976]
49. Nakayama R, Mitani S, Nakagawa T, Hasegawa T, Kawai A, Morioka H, et al. Gene expression profiling of synovial sarcoma: distinct signature of poorly differentiated type. Am J Surg Pathol. 2010; 34(11):1599–1607. [PubMed: 20975339]
50. Kokovic I, Bracko M, Golouh R, Ligtenberg M, van Krieken HJ, Hudler P, et al. Are there geographical differences in the frequency of SYT-SSX1 and SYT-SSX2 chimeric transcripts in synovial sarcoma? Cancer Detect Prev. 2004; 28(4):294–301. [PubMed: 15350633]
51. Wei Y, Wang J, Zhu X, Shi D, Hisaoka M, Hashimoto H. Detection of SYT-SSX fusion transcripts in paraffin-embedded tissues of synovial sarcoma by reverse transcription-polymerase chain reaction. Chin Med J (Engl). 2002; 115(7):1043–1047. [PubMed: 12150740]
52. Bijwaard KE, Fetsch JF, Przygodzki R, Taubenberger JK, Lichy JH. Detection of SYT-SSX fusion transcripts in archival synovial sarcomas by real-time reverse transcriptase-polymerase chain reaction. J Mol Diagn. 2002; 4(1):59–64. [PubMed: 11826189]
53. Fernebro J, Francis P, Eden P, Borg A, Panagopoulos I, Mertens F, et al. Gene expression profiles relate to SS18/SSX fusion type in synovial sarcoma. Int J Cancer. 2006; 118(5):1165–1172. [PubMed: 16152617]
54. Inagaki H, Nagasaka T, Otsuka T, Sugiura E, Nakashima N, Eimoto T. Association of SYT-SSX fusion types with proliferative activity and prognosis in synovial sarcoma. Mod Pathol. 2000; 13(5):482–488. [PubMed: 10824918]

55. Xu Z, Yang T, Wu B, Zhong H, Yang Z, Zhou B, et al. [Detection and analysis of SYT-SSX fusion gene in synovial sarcoma]. Zhonghua Bing Li Xue Za Zhi. 2001; 30(6):431–433. [PubMed: 11866985]

56. Billings SD, Walsh SV, Fisher C, Nusrat A, Weiss SW, Folpe AL. Aberrant expression of tight junction-related proteins ZO-1, claudin-1 and occludin in synovial sarcoma: an immunohistochemical study with ultrastructural correlation. Mod Pathol. 2004; 17(2):141–149. [PubMed: 14704716]

57. Tvrdik D, Povysil C, Svatosova J, Dundr P. Molecular diagnosis of synovial sarcoma: RT-PCR detection of SYT-SSX1/2 fusion transcripts in paraffin-embedded tissue. Med Sci Monit. 2005; 11(3):MT1–MT7. [PubMed: 15735574]

58. Li C, Hung Wong W. Model-based analysis of oligonucleotide arrays: model validation, design issues and standard error application. Genome Biol. 2001; 2(8) RESEARCH0032.

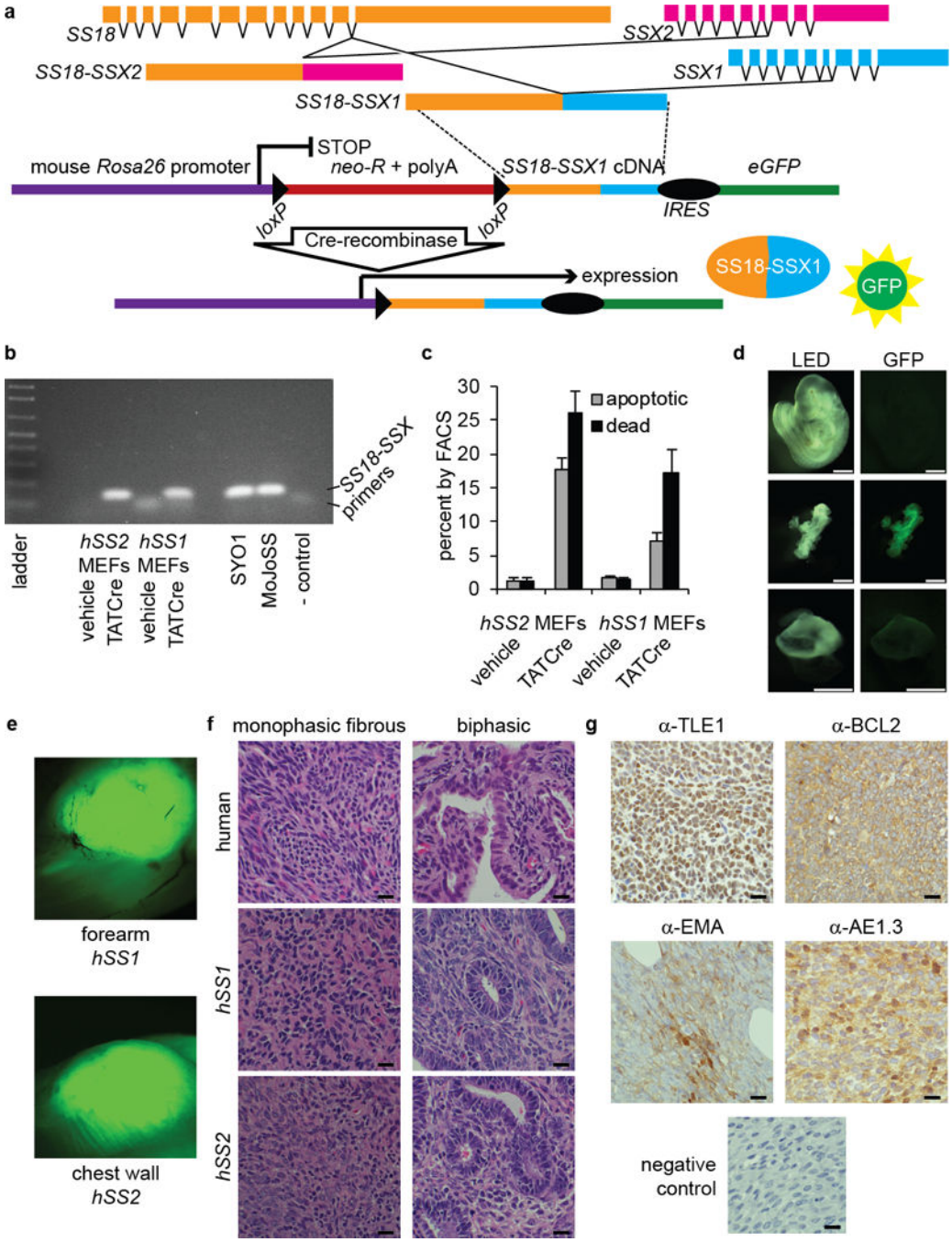

Figure 1. Comparable synovial sarcomagenesis from *SS18-SSX1* and *SS18-SSX2*

(a) Schematic of the derivation of both fusion oncogene transcripts *SS18-SSX2* and *SS18-SSX1*, showing the insertion of the latter into a *Cre-loxP* conditional expression vector at the *Rosa26* locus. Cre-mediated recombination excises the stop sequence, enabling tandem expression of the fusion oncogene and the enhanced green fluorescent protein (*eGFP*) from an internal ribosomal entry site (*IRES*).

(b) Reverse transcriptase polymerase chain reaction (RT-PCR) with type-non-specific *SS18-SSX* primers, showing expression 16 hours following administration of TATCre protein, but

not vehicle control, in both *hSS2* and *hSS1* mouse embryonic fibroblasts (MEFs) *in vitro*. Positive controls include the *SS18-SSX2*-expressing SYO1 and *SS18-SSX1*-expressing MoJo human synovial sarcoma cell lines.

(c) Fluorescence associated flow cytometry demonstrates increased apoptotic and dead cell fractions 72 hours following TATCre administration compared to controlled conditions in *hSS1* and *hSS2* MEFs *in vitro*.

(d) Most *HprtCre*-positive embryos heterozygous for *hSS1* (middle) or *hSS2* (lower) were already resorbed, but residual GFP+ tissue was retrieved at embryonic day 9.5 from one embryo each and compared to Cre-negative littermate controls (top).

(e) GFP fluorescence photos of tumors arising in *hSS1* and *hSS2* mice bearing *Myf5Cre*.

(f) Representative hematoxylin and eosin histopathology demonstrates monophasic fibrous (MSS, left) and biphasic glandular and fibrous (BSS, right) areas in human and mouse *hSS1* and *hSS2* derived tumors. (Scale bars are 10 μm in length)

(g) Immunohistochemistry showing classic nuclear TLE1, cytoplasmic BCL2, and the typical, patchy epithelial membrane antigen (EMA) and pancytokeratin (AE1.3) staining in *hSS1* derived tumors. (Scale bars are 10 μm in length)

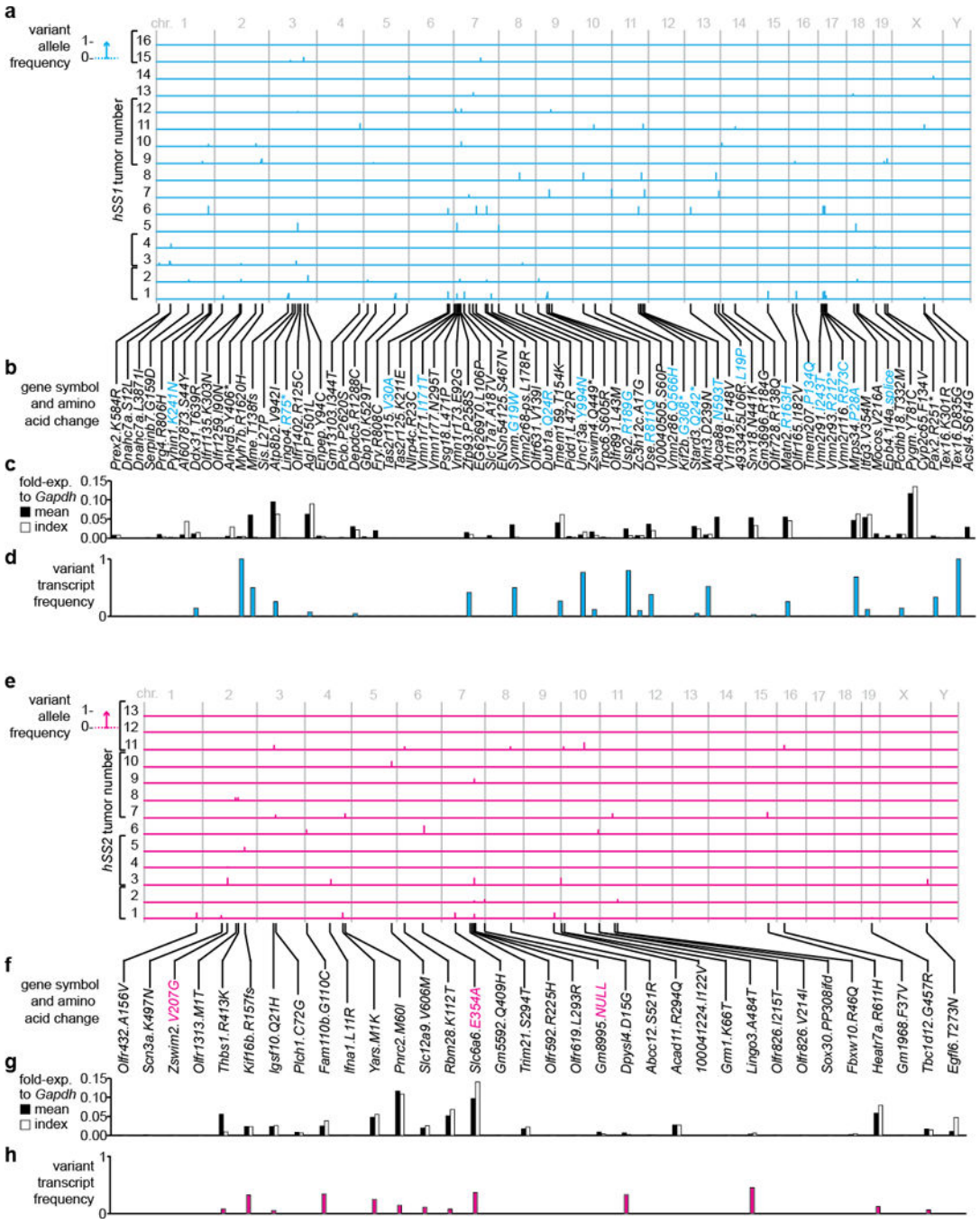

Figure 2. Whole exome sequencing of mouse synovial sarcomas demonstrates few mutations

(a) The variant allele fraction (VAF) for each mutation is plotted as upward deviation on the ordinate axis (scale to the left) plotted against the genomic location along the abscissa. Each of 16 *Myf5-Cre;hSS1* tumor genomes is presented as a separate plot. (Brackets indicate which tumors arose in the same mouse.)

(b) List of the gene impacted and amino acid change associated with each mutation. (Cyan colored gene symbols indicate VAF ≥40).

(c) Plot of the mean fold-change expression relative to *Gapdh* of the gene associated with each mutation across all the tumors (black column) as well as its expression in the mutation-bearing (index) tumor (white column).

(d) Plot of the variant transcript frequency (VTF), or the fraction of mutated transcript reads over total transcripts reads that cross the mutation site in the index tumor.

(e) Mutations plotted for the genome of each of 13 *Myf5-Cre;hSS2* tumors.

(f) Gene list for *hSS2* tumor mutations. (Magenta colored gene symbols indicate VAF ≥40).

(g) Expression of genes involved by *hSS2* tumor mutations.

(h) Fraction of mutated transcript reads in each index *hSS2* tumor.

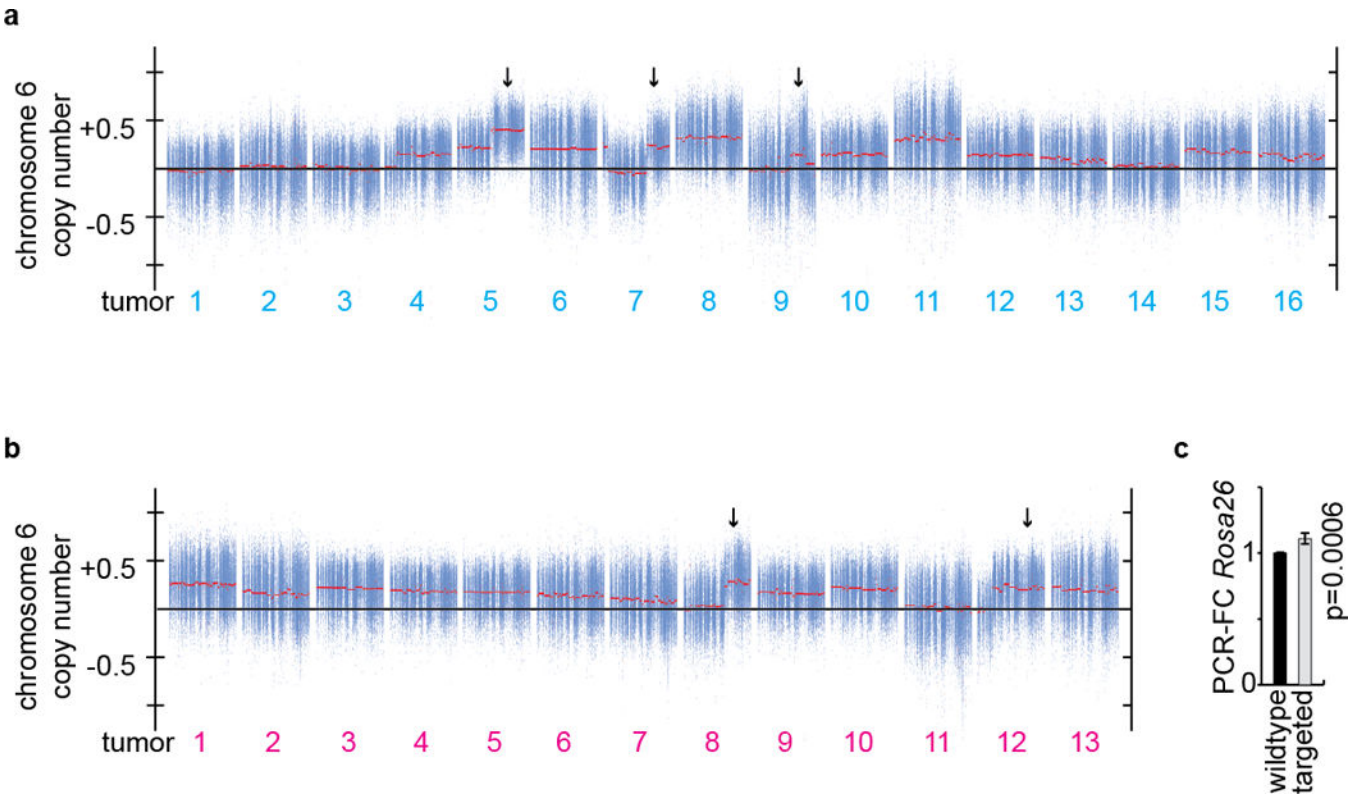

Figure 3. Copy number analysis shows amplification of the fusion expression locus

(a) Plots of copy number variation for mouse chromosome 6 in 16 *Myf5-Cre;hSS1* tumors relative to germline control DNA. (Arrows indicate the position of the *Rosa26* locus in each tumor with partial amplification of chromosome 6.)

(b) Plots of copy number variation for mouse chromosome 6 in 13 *Myf5-Cre;hSS2* tumors.

(c) Plot of the mean prevalence (±SD) of the PCR product of the targeted *Rosa26* allele relative to the wildtype *Rosa26* allele; the gain was in the targeted allele in all cases assessed (n = 8, p-value from Student's t-test).

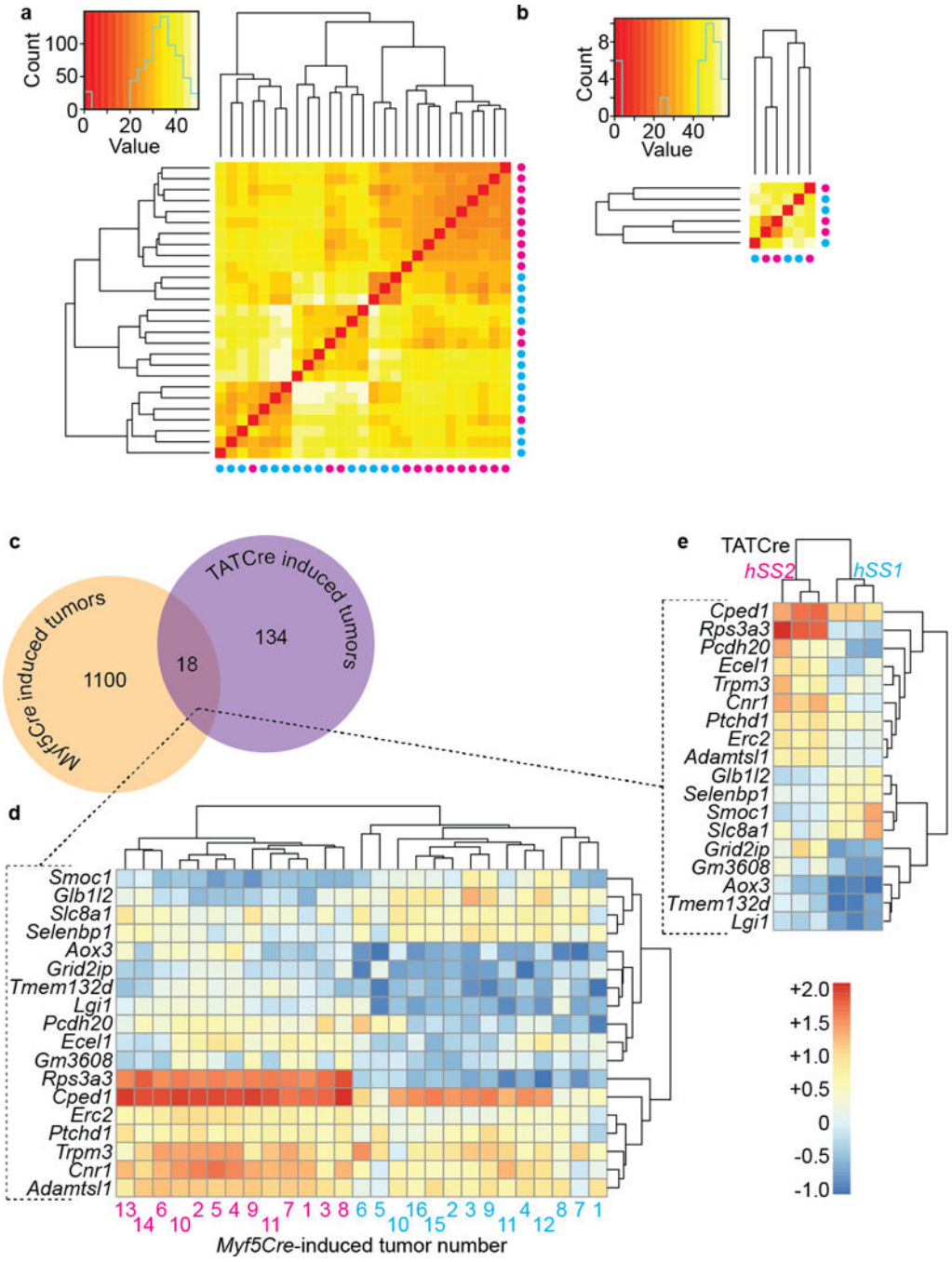

Figure 4. Synovial sarcoma transcriptomes differ minimally by fusion genotype

(a) Heatmap of unsupervised hierarchical clustering of samples by FPKM values generated from sequencing of total RNA from tumors induced in mice by *Myf5-Cre* activation of either *hSS1* (cyan) or *hSS2* (magenta). Samples are listed as tumor numbers.

(b) Heatmap of unsupervised hierarchical clustering by FPKM of TATCre-induced tumors.

(c) Venn diagram of the genes 2-fold and significantly ($p < 0.05$) differentially expressed in 14 *hSS1* and 13 *hSS2* tumors initiated by *Myf5Cre*, then 3 of each genotype initiated by TATCre injection into the hindlimb.

(d) Unsupervised hierarchical clusterings of *Myf5Cre*-induced *hSS1* and *hSS2* tumors with heatmap demonstrating the log10 transformed FPKM expression values for genes selected by 2-fold and significant differential expression across both cohorts of mouse tumors by fusion type.

(e) Similar clustering with heatmap for the TATCre injection-induced tumors.

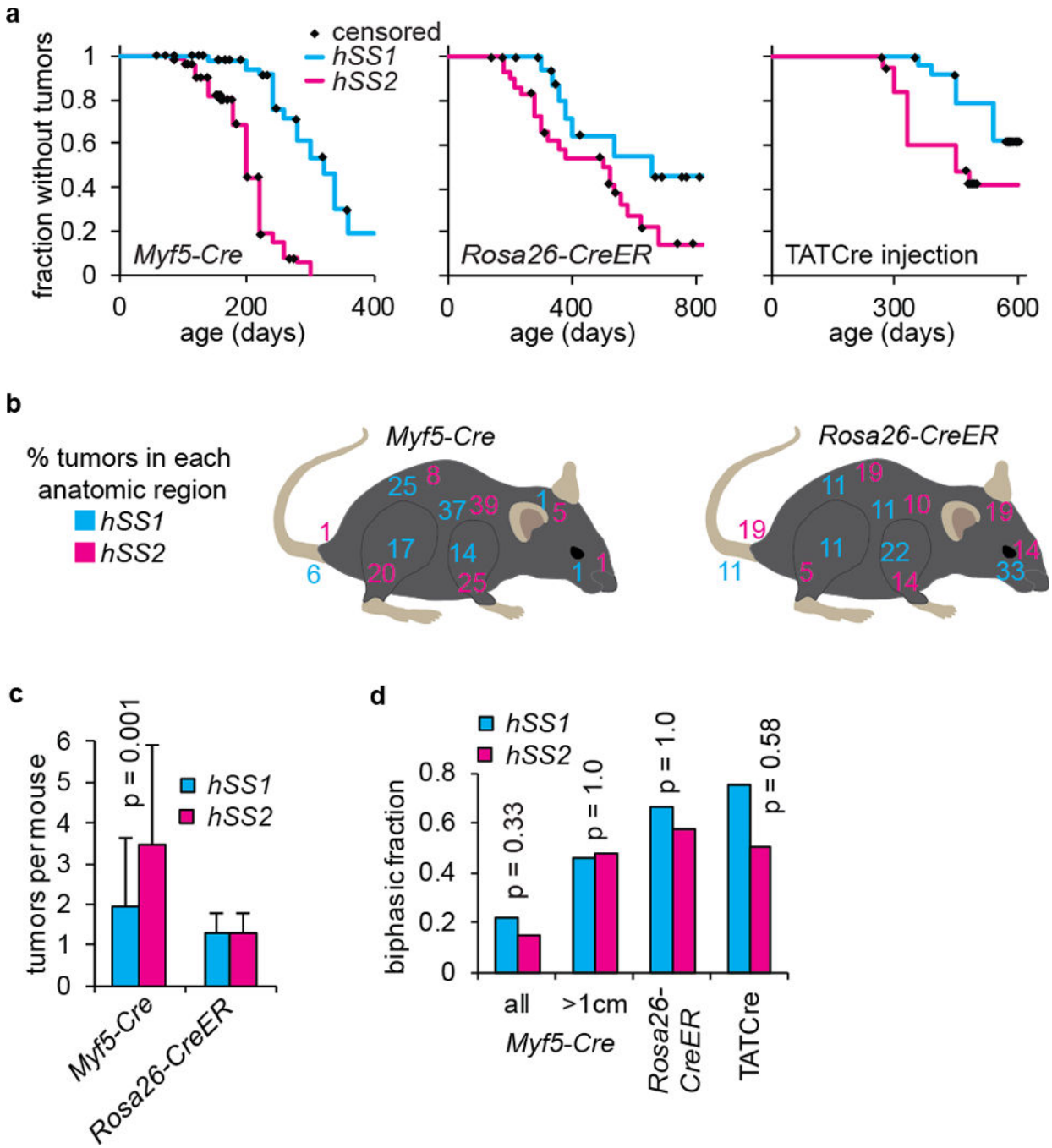

Figure 5. Comparable sarcomagenesis between *SS18-SSX1* and *SS18-SSX2*

(a) Plot of the non-morbid fraction of mice bearing *Myf5-Cre* (left) or *Rosa26-CreER* (right) and either *hSS1* (n = 57 and 17) or *hSS2* (n = 122 and 31) against age in days.

(b) Percentage of tumors in each anatomic location (tail, back, chest wall, hindlimb, forelimb, head, face) in mice of the *Myf5-Cre* (*hSS1* n = 82, *hSS2* n = 166) and *Rosa26-CreER* (*hSS1* n = 9, *hSS2* n = 21) genotypes.

(c) Mean number of tumors per mouse among 41 *Myf5-Cre;hSS1* and 48 *Myf5Cre;hSS2* mice with error bars demonstrating the standard deviations (p-value from Student's t-test).

The mice of *Rosa26-CreER* genotypes had samples of 7 and 14, respectively for *hSS1* and *hSS2*.

(d) The relative prevalence of BSS histology among all *Myf5-Cre*-induced tumors or the subset of tumors greater than 1 centimeter (samples of 41 total and 13 large *hSS1* tumors and 123 total and 19 large *hSS2* tumors, p-values represent two-tailed Fisher exact test). Also presented are the comparison of BSS fraction among tumors induced by *Rosa26-CreER* (*hSS1* n = 6, *hSS2* n = 14) and TATCre (*hSS1* n = 4, *hSS2* n = 10).

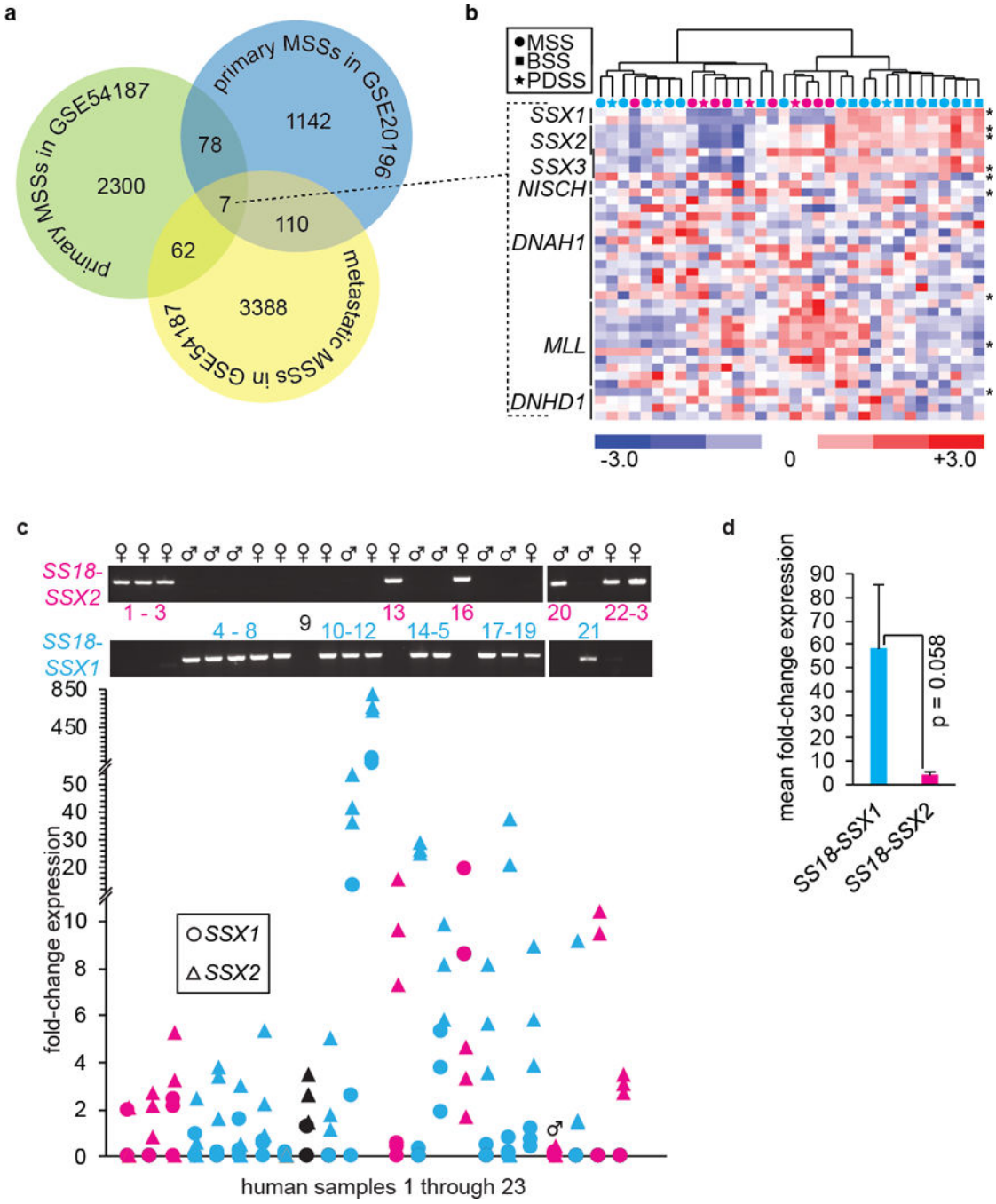

Figure 6. Human *SS18-SSX1* and *SS18-SSX2* synovial sarcomas differentially express *SSX* genes

(a) Venn diagram of differentially expressed genes (t-test $p < 0.05$) shared between 3 groups of human synovial sarcomas previously profiled by cDNA microarray.

(b) Cluster heatmap of one group of samples and all probes for the 7 genes differentially expressed in all three groups. (*indicates p-value < 0.5 differences between expression in the two tumor genotypes that was shared by the other samples in significance and direction of change.)

(c) Gel image demonstrating RT-qPCR to determine the presence of each fusion gene in 23 human synovial sarcoma samples, over the corresponding plot of RT-qPCR GAPDH-normalized fold-change expression levels (relative to *SSX1* in testis) of native *SSX2* (triangles) and *SSX1* (circles), with cyan representing *SS18-SSX1* tumors and magenta *SS18-SSX2* tumors). Sample 9 demonstrated neither *SS18-SSX1* nor *SS18-SSX2* expression. Sample 20 (annotated below with an additional male symbol), the only *SS18-SSX2* tumor from a male, was also the only tumor with negligible native *SSX2* expression. **(d)** Mean ± S.E.M. of the RT-qPCR-determined SSX2 expression for each human tumor fusion genotype. P-value is from two-tailed Student's t-test.

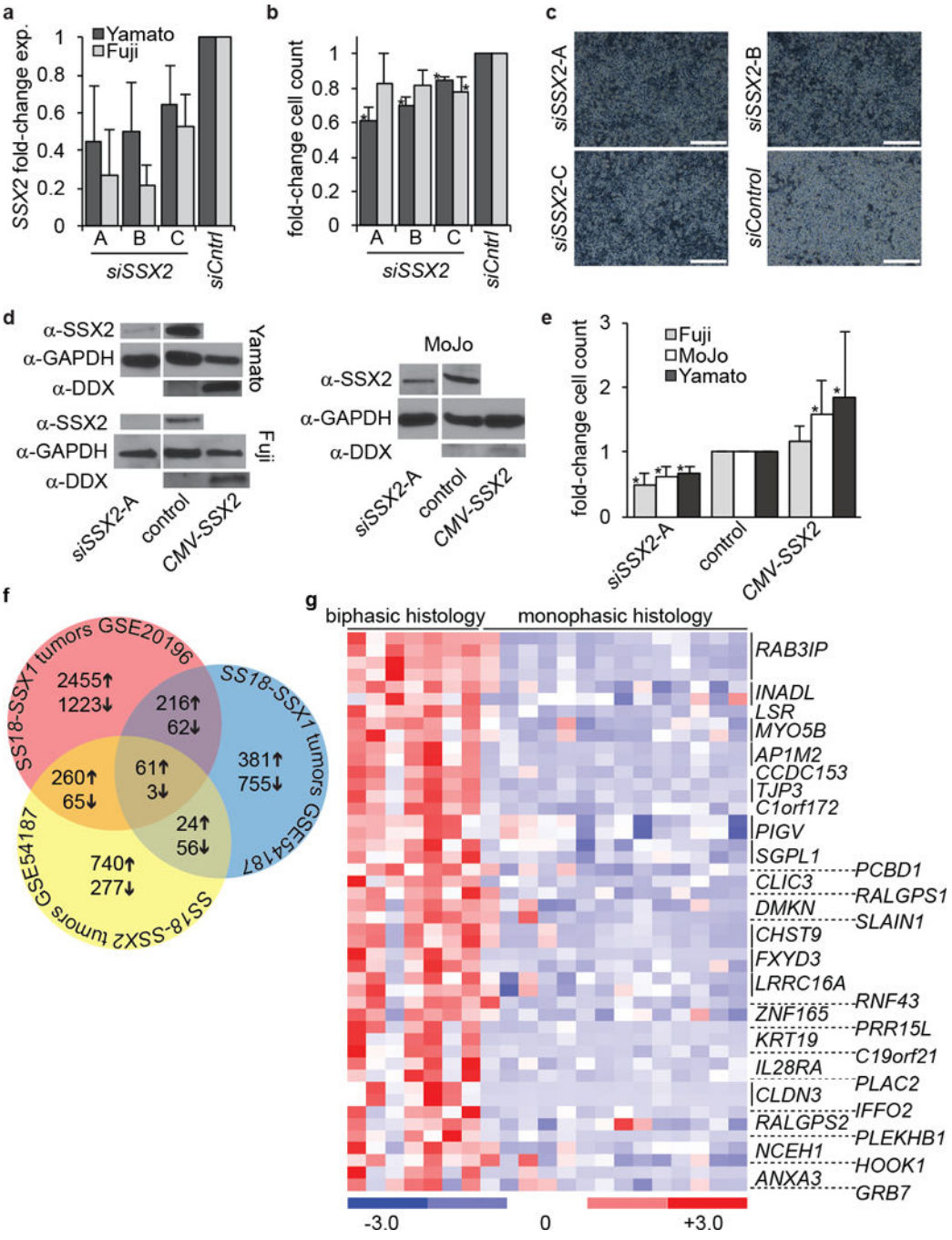

Figure 7. Possible roles for *SSX2* in synovial sarcoma

(a) Mean ± SD GAPDH-normalized Western densitometry measurements of *SSX2* knockdown by three different siRNAs in human cell lines Fuji and Yamato, (exp. = expression; n = 3 biological replicates; experiment repeated).

(b) Mean fold-change ± SD in cell count 72 hours after application of siRNA (n = 3 biological replicates; experiment repeated).

(c) Representative photomicrographs of cell density 72 hours after application of siRNA to the Fuji cell line (scale bars = 400 μm).

(d) Westerns of SSX2 or its tag (DDX) 48 hours after transfection of an *SSX2* overexpression vector (*CMV-SSX2*), an *SSX2* siRNA, or control conditions.
(e) Fold-changes in mean ± SD cell counts to measure proliferation 48 hours after transfection of an *SSX2* overexpression vector (*CMV-SSX2*), an *SSX2* siRNA, or control conditions. (* indicates two-tailed Student's t-test p-value < 0.05; biological replicates per cell line: Fuji n = 5, MoJo n = 9, Yamato n = 6).
(f) Venn diagram of the numbers of unique genes differentially expressed to a significance of $p<0.05$ between biphasic and monophasic tumors in each group and shared between groups. Up arrows indicate genes relatively upregulated in biphasic tumors. Down arrows indicate genes relatively downregulated in biphasic tumors.
(g) Heatmap of microarray expression values of genes that were significantly upregulated in all three tumor cohorts, here presented in the GSE20196 cohort of SS18-SSX1-expressing tumors.

Table 1

Testing for gender-specific prevalences of each fusion genotype in synovial sarcomagenesis.

Study	*SS18-SSX1*		*SS18-SSX2*	
	Male	**Female**	**Male**	**Female**
Ladanyi, et al., 2002	73	72	31	56
Guillou, et al., 2004	61	51	19	34
Amary, et al., 2007	34	35	20	21
Sun, et al., 2009	32	18	47	44
Takenaka, et al., 2008	31	37	13	27
Ren, et al., 2013	27	20	29	12
Messelani, et al. 2001	21	19	7	17
Nakayama, et al., 2010	11	12	3	8
Fernebro, et al., 2006	8	4	5	4
Koković, et al., 2004	7	10	15	15
Inagaki, et al., 2000	6	4	2	7
Tvrdík, et al., 2005	4	1	0	2
Total	315	283	191	247

2×2 contingency:	*SS18-SSX1*	*SS18-SSX2*	**total**
Male	315	191	**506**
Female	283	247	**530**
total	**598**	**438**	1036
		Ratio	**1.44**
		Fisher exact test	**p = 0.0046**